ARCHIVES
of
FOUNDRY ENGINEERING

10.24425/afe.2026.158007

Published quarterly as the organ of the Foundry Commission of the Polish Academy of Sciences

ISSN (2299-2944)
Volume 2026
Issue 2/2026

199 – 205

24/2

Solidification of Massive Nodular Cast Iron Mill Rolls in Combined Metal–Sand Molds

V. Khrychikov [a], O. Semenov [b], Y. Aftandiliants [c], S. Gnyloskurenko [c,] *, H. Meniailo [a], T. Semenova [a]

[a] Ukrainian State University of Science and Technologies, Ukraine
[b] Progress-tech, Ukraine
[c] Physico-technological Institute of Metals and Alloys, National Academy of Sciences of Ukraine
* Corresponding author: E-mail address: slava.vgn@gmail.com

Received 25.11.2025; accepted in revised form 30.03.2026; available online 14.07.2026

Abstract

At crystallization of castings the various defects such as shrinkage cavities, shrinkage depressions and others are often formed. The purpose of the present work is to experimentally investigate the crystallization process of a massive rolling mill of high-strength cast iron, and to adapt the mathematical model. In the result of the experimental study of the 2160 kg mill roll casting solidification process, the mathematical model was adapted from a reference roll to enable its application to rolls of other sizes. Simulation of ≈7500 kg rolls solidification in combined metal–sand molds revealed the position of the isosolidus fronts, formation of a shrinkage depression on the hot top surface after electroslag heating, and the volume of shrinkage cavities in the hot spot. The volume of the depression was used as the first approximation to estimate the volume of the shrinkage cavity in the hot spot of the casting. This method enables the calculation of chill mass and the elimination of hot spots and shrinkage depressions without the need for complex measuring equipment.

Keywords: Casting, Nodular cast iron, Shrinkage defects, Hot spot, Low pressure

1. Introduction

At castings crystallization the various defects such as shrinkage cavities, hot cracks, gas porosity, liquation, shrinkage depressions, and others are often formed [1,2]. To prevent the formation of shrinkage defects, risers are used to feed the solidifying metal. They are located above the hot spot, where solidification occurs later than in the rest of the casting. To eliminate shrinkage cavities in this area, various techniques are applied to extend the solidification time of the riser [3]. However, shrinkage depressions is often formed on the surface of the riser and the casting and characterized by surface indentations with rounded edges, caused by metal contraction during solidification [1].

The formation of this defect (Fig. 1a) was previously investigated [4]. Low pressure in the shrinkage cavity located below the shrinkage depression was predicted, although it was not experimentally measured. To reduce the defect a side core and insulation to the hot top surface were proposed. The unique experiments on the measurement of low-pressure during feeding of nodular and flake graphite cast iron were first described in [5]. In castings sized 101.6 × 101.6 × 294 mm with a 76.2 mm riser, two quartz tubes (≈7 mm in diameter) were inserted into the hot spot. A U-shaped water manometer was used to measure the pressure. No low pressure was recorded in gray iron castings, but it was detected in nodular graphite iron. As a result, the authors recommended enlarging the risers for ductile iron. No shrinkage depressions were observed in those experiments [5].

To improve the experimental method, a device was developed [6,7] using a medical spinal needle made of stainless steel (Ø 0.7 mm, with a 0.44 mm internal diameter), which prevents molten metal penetration and minimizes influence on metal

© The Author(s) 2026. Open Access. This article is licensed under a Creative Commons Attribution 4.0 International License (http://creativecommons.org/licenses/by/4.0/), which permits use, sharing, adaptation, distribution and reproduction in any medium or format, as long as you give appropriate credit to the original author(s) and the source, provide a link to the Creative Commons licence, and indicate if changes were made.

crystallization. It was shown that the reason of shrinkage depressions (1 in Fig. 1) is the formation of a hot spot (2), from which molten metal is filtered to feed the solidifying casting in nearby regions. As the melt moves from the center a shrinkage cavity (2) and low pressure (P_o) are formed. Consequently, atmospheric pressure (P_{at}) causes the collapse or distortion of the solidified shell (1) on the casting surface where strength is the lowest [7]. It is also important to mention, that the low-pressure zone is created in the liquid area isolated from the feeding by a solid phase barrier.

In foundries, internal shrinkage cavities and hot spots cannot always be reliably detected using X-ray-based methods (radiographic, electro-radiographic, radioscopic, or radiometric) [8]. Ultrasonic testing (UT) requires surface preparation to a roughness of $R_a \leq 12.5\text{-}6.3$ µm [9], and a special coupling medium must be used for reliable signal transmission. As a result, primary casting inspection is often visual, but if a shrinkage depression is present, the internal shrinkage cavity size remains unknown.

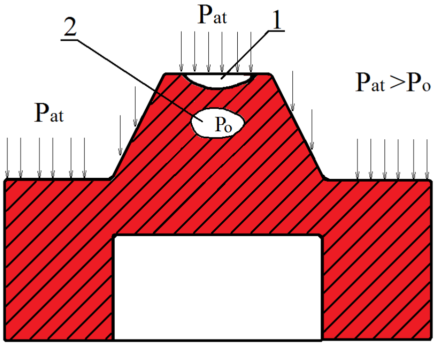

Fig. 1. Typical appearance of a shrinkage depression (1) adjacent to the hot spot and shrinkage cavity (2):
Pat – atmospheric pressure; P_o – low pressure inside the shrinkage cavity

Modern simulation software cannot precisely model heat removal from a casting into the mold, the effects of convection in the melt and mushy zone, thermal contact, radiative transfer, or the shrinkage gap between a casting and mold. Thermophysical properties are generally taken from literature data measured under laboratory conditions [10, 11]. For instance, the advanced 3D model capable of predicting shrinkage defects as a function of interacting physical phenomena including free-surface flow, heat transfer, and solidification allows to distinguish surface shrinkage and internal porosity [10]. However, the authors note that no commercial software currently reproduces the solidification process with full consideration of all temperature-dependent thermophysical parameters.

Thus, the experimental study of solidification is essential for adapting mathematical models and generating reliable reference simulations that can be scaled to various casting sizes. But such studies are limited to the specific Fe-C alloys due to their labor-intensity [12]. Particularly it was done for nodular cast iron mill rolls cooled in combined metal–sand molds.

The purpose of the present work is to experimentally investigate the crystallization process of high-strength cast iron in a massive rolling mill, to adapt the mathematical model and to estimate the volume of the shrinkage cavity in the thermal unit of the casting in relation of the shrinkage depression volume.

2. Experimental methods

The assessment of the size of the shrinkage depression was carried out on rolling rolls in the conditions of the Dnipro Roll Plant (DZPV) using the plant measuring devices that have passed the state metrological control. The study of the shrinkage defects distribution was carried out after mechanical processing of the rolls using ultrasonic flaw detectors UD4-76 and the DATAMES COMBI installation, which was located on the rolling lathe.

The solidification of rolling mill rolls was studied using modeling according to [13], which makes it possible to:

1. Sequentially vary the power and duration of heating of the metal melt surface (electroslag heating) during the solidification of the casting.
2. Modify the kinetics of latent heat release during crystallization within the crystallization temperature range, taking into account the fraction of solid phase formed at the liquidus and solidus temperatures.
3. Introduce a correction that accounts for the release of phase transformation heat during the eutectoid transformation. Its magnitude and the temperature interval of heat release were determined based on the results obtained from the experimental cooling curves.
4. Take into account changes in the shrinkage gap during solidification of the casting in a chill mold, depending on the thickness of the solidified metal layer.

In the computational domains the temperature field and the solidification front were determined in accordance with the heat conduction equation:

$$\rho(r,z,T)C(r,z,T)\frac{\partial T(r,z,\tau)}{\partial \tau}=\frac{1}{r}\frac{\partial}{\partial r}\left(\lambda(r,z,T)r\frac{\partial T(r,z,T)}{\partial r}\right)+\frac{\partial}{\partial z}\left(\lambda(r,z,T)\frac{\partial T(r,z,T)}{\partial z}\right), \quad (1)$$

where ρ is the density; c is the specific heat capacity; r and z are the radial and axial coordinates of the computational domain; T is the temperature; τ is the time and λ is the thermal conductivity coefficient.

The model is based on the coupled numerical solution of the two-dimensional transient heat conduction equation in the regions of liquid, mushy (liquid–solid), and solid metal, being cooled in a combined casting mold consisting of seven elements with different thermophysical properties, as well as a heat source (Q) providing heating of the upper part of the casting throughout the entire solidification period.

The solidification process is described within the framework of the quasi-equilibrium theory of the two-phase zone. The latent heat of crystallization χ was taken into account using an effective heat capacity coefficient C:

$$C(r,z,T)=\begin{cases} C_{ж} \\ C_{ж}+\frac{\partial \varphi}{\partial T}\chi \text{ if } T_S \leq T \leq T_L, \\ C \end{cases} \quad (2)$$

$\chi=\chi_1+\chi_2+\chi_3$; $\chi_1=\kappa_1\chi$ if $T_1 < T \leq T_L$; $\chi_2=\kappa_2\chi$ if $T_2 < T \leq T_1$;

$\chi_3=\kappa_3\chi$ if $T_S < T \leq T_2$

To improve calculation accuracy in accordance with thermocouple readings, the kinetics of latent heat release during crystallization χ within the liquidus–solidus temperature interval (T_L–T_S) was divided into three regions k_1, k_2, and k_3. In each region, the fraction of the solid phase formed was determined based on the results of experimental measurements of real casting solidification and studies performed using a high-temperature differential thermal analyzer VDTA-8M at heating and cooling rates of 80, 60, 40, and 20 °C/min.

For the investigated cast iron rolls with spheroidal graphite, T_L = 1230 °C and T_S = 1125 °C. The cooling curves calculated using the model approach the experimental ones if 20% of the solid phase forms within the temperature interval 1230–1210 °C; within the solidification interval 1209–1155 °C, 10% of the solid phase and the corresponding latent heat of crystallization are released; and within the eutectic crystallization temperature interval 1154–1125 °C, 70% of the latent heat of crystallization is released. This assumption is justified by the fact that during the solidification of cast iron castings the "thermal arrest" at the solidus temperature is maximal.

For steel castings, on the contrary, it was assumed that the major portion of the latent heat of crystallization is released at the liquidus temperature, which led to a modification of these ratios for each specific chemical composition of the rolls.

Experimental studies [3] revealed accelerated solidification of the lower neck of the rolling mill roll compared to the upper one. In the model, the transport of dendrite fragments into the lower neck was taken into account by reducing the values of the phase transformation heat for a portion of the metal volume located in the lower neck. In addition, a correction was introduced to account for the release of phase transformation heat during the eutectoid transformation.

The boundary conditions at the interface between the roll and the chill mold were determined taking into account the shrinkage gap formed as a result of metal shrinkage, according to the equation:

$$-\lambda_K \frac{\partial T_м}{\partial r} = \lambda_K \frac{\partial T}{\partial r} \frac{1}{\frac{\chi_{кр}}{\lambda_{кр}} + \frac{\Delta}{\lambda_Г}} (T_K - T_M) + \frac{\varepsilon_M \varepsilon_K}{\varepsilon_M + \varepsilon_K - \varepsilon_M \varepsilon_K} G_0 \left[T_K^4 - T_M^4\right], \quad (3)$$

where Δ is the thickness of the gap between the casting and the chill mold; ε is the emissivity; k denotes the chill mold; *m* denotes the roll metal; *f* denotes the sand mold; *n* denotes the lower neck; *g* denotes the gas gap between the casting and the chill mold; *e* denotes the eutectoid phase transformation interval; *a* denotes air; *r* and *z* are the radial and axial coordinates of the computational domain, respectively; the subscript 0 indicates initial values at τ = 0; and *c* denotes the ambient environment

The boundary conditions at the interface between the chill mold and the environment were assumed as follows:

$$-\lambda_к \frac{\partial T}{\partial r} = \alpha_к (T_c - T_к) + \varepsilon_к G_0 \left[T_c^4 - T_к^4\right] \quad (4)$$

where α is the heat transfer coefficient, and G_0 is the Stefan–Boltzmann constant.

Heat exchange at the external boundaries of the other part of the mold with the environment was calculated according to Newton's law using the corresponding values of α. At the interface between the casting and the sand mold, thermal resistance was neglected, since it was assumed that the porous mixture is in close contact with the casting surface, and that hydrogen released from the casting and the sand mold increases the thermal conductivity of the gas in the pores of the mixture to a value close to that of $\lambda_ф$. The thickness of the foundry coating layer and its thermal conductivity coefficient were also taken into account.

Heat transfer from the liquid melt to the solidified layer of the casting (convective mixing) was taken into account using an effective thermal conductivity coefficient (λeff). To determine λeff, the Nusselt, Grashof, and Prandtl criteria were used, and after transformations for the turbulent mixing regime of the melt during pouring, the following expression was obtained:

$$\lambda_{эф} = A_1 \sqrt[3]{\Delta t_n \Delta r} \quad (5)$$

where Δt_n is the metal superheat above the liquidus temperature; Δr is the characteristic dimension (spatial grid step); and A_1 is a proportionality coefficient depending on the thermophysical properties of the alloy

The system of differential equations and boundary conditions was solved using the finite difference method with a locally one-dimensional scheme. In calculations of the solidification of cast iron rolling mill rolls of various sizes in combined metal-sand molds, the initial thermophysical coefficients were adopted in accordance with literature and experimental data. The relative error of the calculated data compared to experimental measurements is 1.4% for the roll barrel with a diameter of 450 mm at the end of solidification at 80 minutes, 1.3% for the lower neck with a diameter of 330 mm at 130 minutes, and 0.9% for the upper neck with a diameter of 330 mm at 180 minutes. The developed model was adapted based on experimental temperature measurement data corresponding to the end of the solidus thermal arrest at the center of the cylindrical casting.

Thus, the calculated cooling curves were in good agreement with the experimental ones, which made it possible to use the mathematical model for rolling mill rolls of various sizes produced by the Dnipropetrovsk Roll Plant and to establish heat input regimes to the molten metal surface of the riser in order to improve the efficiency of electroslag heating of the riser.

The solidification of a 2160 kg nodular cast iron roll was studied using chromel–alumel thermocouples type K (Ø 0.5 mm) rated for short-term measurement up to 1370 °C [12]. The thermocouple hot junction (Fig. 2, pos. 8) was protected by a quartz tube (2), a thin-walled stainless-steel sleeve (3), and further secured by a bushing (6) and wedges (7) to prevent hydraulic ejection from the metal mold (1) due to molten metal pressure.

Thermocouples were calibrated against a reference platinum thermocouple and insulated using high-alumina dual-channel ceramic tubing (Ø 2.5 mm, with 0.65–0.75 mm internal channel diameters). Compensation wires were not used; cold junctions were directly connected to a KSP-4 potentiometer (accuracy class 0.25, range 700–1370 °C, measurement interval 4 s). The overall permissible measurement error was ±2.5 °C.

Cast iron was melted in an IIC-6/2.5 crucible induction furnace, treated with magnesium at 1370 °C, and poured at 1320 °C over 42 seconds into a mold with dimensions (in mm): lower neck

Ø276…327, height 920; chill mold Ø450, height 800; upper neck + riser Ø330, height 1200. Sand-clay molds for the necks and riser, chill preparation, tangential gating system for bottom, and mold assembly were carried out at Dnipro Roll Plant according to the standard procedure [3]. Chemical composition of the roll is (wt %): C – 3.09; Si – 1.41; Mn – 0.53; P – 0.196; S – 0.008; Cr – 0.32; Ni – 0.90; Mg – 0.04.

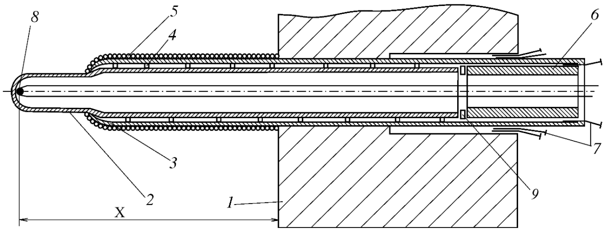

Fig. 2. Protective assembly for thermocouple installation in molten metal:
1 – cast iron chill mold; 2 – quartz tube with extended tip for thermocouple junction; 3 – rolled stainless steel sleeve; 4 – thermal insulation cord in air gap; 5 – insulation layer; 6 – bushing to fix the quartz tube in place; 7 – wedging pins; 8 – thermocouple hot junction; 9 – compensator for quartz tube thermal expansion; X – distance from mold inner wall to thermocouple junction

During electroslag heating (ESH) of the rolls, the temperature of the slag bath was measured with a tungsten-rhenium (WR) thermocouple. The hot junction was laser-welded (Kvant-12) and enclosed in a quartz tip (Ø 7.0 mm outer, Ø 4.0 mm inner).

3. Results and discussion

Figure 3a presents cooling curves from thermocouples positioned at distances of 225, 150, 90 and 17 mm from the inner wall of a Ø450 mm chill mold. Within one minute after pouring 2160 kg of molten metal, its temperature decreased by 90 °C, from t_P = 1320 °C to t_0 = 1230 °C, due to intensive mixing of the melt in the casting mould, the temperature of which was 95 °C before the start of pouring.

As early as the third minute, thermocouple No. 1 (see Fig. 3a) recorded undercooling to a temperature of t_h = 1116 °C, and only then registered an increase in temperature to t_L = 1220 °C along with the release of part of the latent heat of crystallization. Solidification at liquidus ends at 18 min.

The liquidus temperature (t_L = 1220 °C) recorded at 150 mm, 90 mm and shows a thermal plateau at 17 mm. The isotherm progression slows down initially (τ_1, Fig. 3b) but accelerates again after 26 min (isotherm 1210 °C). As cooling continues solidification accelerates in the axial zone (1170 °C isotherm, τ_2–τ_5, Fig. 3b).

The eutectic crystallization temperature at the casting center was t_S = 1115 °C significantly below standard Fe–C diagram values (1147–1153 °C), attributed to magnesium modification, as established in early studies on spheroidal graphite cast iron. Due to accelerated cooling solidus temperature was not recorded by thermocouples 3 and 4, and thus was determined from curve 1. Accordingly the temperature field obtained by minute 5 (Fig. 3c), 100% solid phase is recorded at 17 mm depth; at 30 min – at 97 mm; and by 70 min no liquid phase remains in the Ø450 mm roll barrel.

Cooling curves from Ø450 mm barrels and Ø330 mm necks were used to calibrate thermophysical coefficients in the model [13] for a 2160 kg reference roll of iron with nodular graphite.

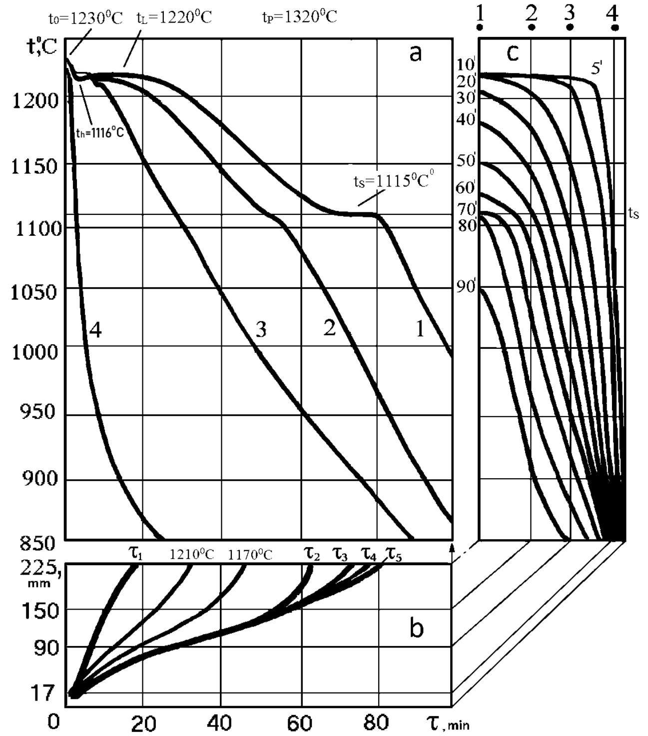

Fig. 3. Cooling curves 1,2,3,4 from thermocouples at distances of 225, 150, 90, 17 mm from the cooling surface (a); Solidification kinetics and isotherms 1210 °C, 1170 °C (b); Temperature fields (c) of the roll barrel at 5, 10, 20, 30, 40, 50, 60, 70, 90 min: t_P – temperature of the molten iron in the ladle before the start of pouring; t_0 – temperature of the molten iron in the mould after pouring; t_h –supercooling temperature; t_L and t_S – liquidus and solidus temperatures, respectively; τ_1 – end of the liquidus temperature "stop"; τ_2, τ_4 – start/end of solidus plateau; τ_3 – 50% solid phase based on lever rule; τ_5 – end of solidification (100% solid phase)

Application Example. At the 550-2 mill at Dnipro Metallurgical Plant (DMZ), conic bearings are used instead of cylindrical ones, while the roll pass grooves remain cylindrical. Thus, the roll barrel is Ø732 mm with conical upper and lower necks and cylindrical pass grooves of Ø305 mm (lower) and Ø336 mm (upper). The upper neck and riser reach 1944 mm in height; gross roll mass ≈7500 kg. According to the technological standards of the foundry shop, the height of the feeder head is 600 mm and it is formed in a flask with a height of 648 mm (Fig. 4a).

Following complaints from DMZ the modeling of roll solidification of iron with nodular graphite revealed premature solidification of the hot top surface. Despite the use of exothermic insulation and superheated molten iron, a solid shell formed by 30 min (30^{I} in Fig. 4a), resulting in low pressure in the enclosed liquid–mushy zone, reduced melt feeding and formation of a large hot spot with shrinkage defects in the upper neck, barrel, and part of the lower neck (see Fig. 4a).

To eliminate defects, the various electroslag heating modes of the riser were simulated, ranging from minimum to maximum power and heating durations equal to or exceeding the roll solidification time (see Fig. 4a). However, due to the roll design, defects cannot be entirely eliminated. Even accelerated cooling of the barrel in the chill mold does not ensure directional solidification from the bottom to the top.

Figure 4b shows one simulated mode of solidification for a nodular graphite cast iron roll. Maximum heating power for 229 minutes ensures formation of a metal bath, from which liquid metal is fed into the lower zones. However, by the 180th minute 100% solid phase forms in the axial area of the upper neck, interrupting the shrinkage feeding from the riser.

Even continued heating at reduced power until 250 minutes maintains the metal bath for another 30 minutes (until 280 min), but this does not eliminate previously formed shrinkage defects. Extending heating beyond 180 minutes is inefficient due to a growing temperature difference between the slag bath (1550 ± 5 °C) and the lower neck, leading to the residual thermal stresses.

The chemical composition of the two rolls produced by the conventional and the proposed technologies was as follows (wt.%): C – 2.96; Si – 1.72; Mn – 0.56; P – 0.184; S – 0.012; Cr – 0.38; Ni – 1.43; Mg – 0.04. After machining, the rolls were subjected to ultrasonic testing using various flaw detectors. The defect size was approximately 5 mm in the axial zone of the roll produced by the conventional technology when an exothermic mixture and double topping-up of the riser with superheated molten iron from an induction furnace were used; slag–metal mixture residues were observed at the riser head (Fig. 5a).

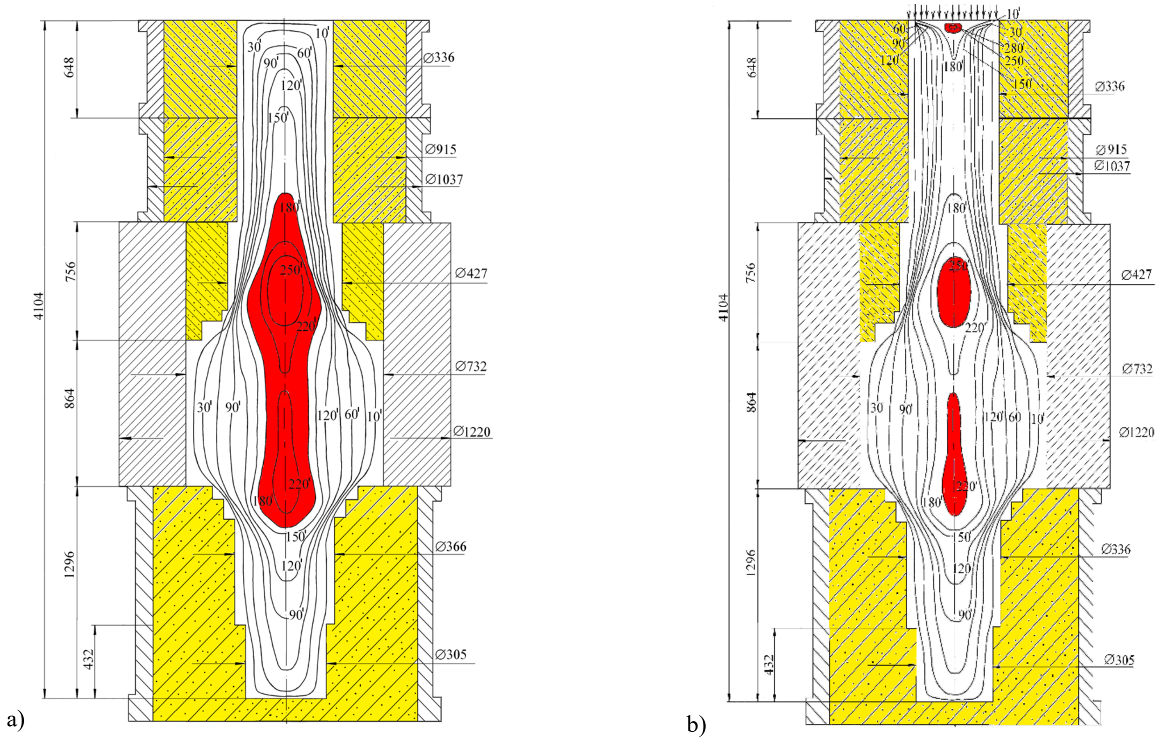

Fig. 4. Numerical simulation of solidification of a cast-iron work roll of ≈7500 kg in a combined metal–sand mold according to DZPV technology (a) and heating of the riser hot top surface (b) at 15 kW from 1 to 229 min, and 5 kW from 230 to 250 min

Nevertheless, the heating significantly reduced the thermal hotspot volume, and the shrinkage defects were confined within isosolidus curves in the upper neck (see 250^{I}), the barrel (220^{I}), and partially in the lower neck. It is important to note that the upper neck is non-driven and does not work under compression. Shrinkage defects in the barrel are located axially, where tangential stresses are minimal. Those in the upper part of the lower neck correspond to tapered bearings and are subject to low mechanical stress during rolling. Thus, the electroslag heating was developed and implemented (see Fig. 4b), consisting of a high-power phase up to 90 min and a reduced-power phase until 180 min.

Verification of the proposed heating modes for rolls of the 550-2 mill was conducted on site at the Dnipro Metallurgical Plant foundry. After machining, ultrasonic testing with various flaw detectors confirmed maximum defect sizes of ≈2 mm. In contrast, for risers heated only by exothermic mixtures and dual topping-up with overheated metal from the induction furnace (Fig. 5a), defects reached ≈5 mm. The observed defect distribution matched simulation results (see Fig. 4a, b). Electroslag heating regimes eliminated roll failures during operation on the rolling mill.

The electroslag process ensures a uniform slag bath temperature of 1550 ± 5 °C. During solidification and metal level drop in the mold, the metal layer at the riser's edge remelts, creating a flat riser top (Fig. 5b). However, on 550-2 mill rolls, shrinkage depressions (Fig. 5c) appear, unlike in other electroslag-heated rolls. As it was experimentally established [7], the shrinkage depression indicates a pressure drop in the thermal node, which is located below the depressions, in the middle of the casting and is not visually detected. The scheme of the processes of electroslag heating of rolls without thermal nodes with a flat surface riser is shown in Fig. 6a and with shrinkage defects 4, shrinkage depression 3 in the metal bath 5 in Fig. 6b.

a b c

Fig. 5. Riser top after dual topping-up with overheated metal and exothermic mixture (a), after ESH in serial production (b), and with shrinkage depression after ESH in 550-2 mill roll (c)

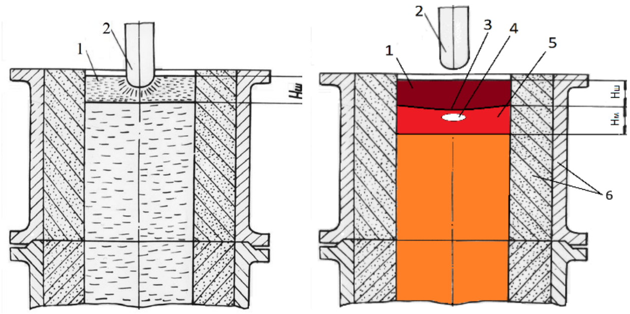

a b

Fig. 6. Electroslag heating of riser: (a) without shrinkage defects; (b) 550-2 roll with shrinkage depression (3):
1 – slag bath; 2 – graphite electrode; 4 – shrinkage cavity; 5 – metal bath; 6 – feeder head mold

Radiographic or ultrasonic inspection of massive castings is often difficult, and the size of hidden cavities under shrinkage depressions is unknown in castings. Therefore, it was proposed to estimate the shrinkage cavity volume in the thermal hotspot of a cylindrical casting, as a first approximation, based on the measured depression volume using the 550-2 roll as an example.

After ESH (see 250^{I} in Fig. 4b), the shrinkage depression appears as a spherical cap (Fig. 7) with height h, measured on the roll. The base radius r equals the riser radius. The spherical segment volume is then calculated using the well-known formula:

$$V = \pi/6 \cdot h\ (h^2 + 3r^2) \tag{6}$$

At a riser radius $r = 168$ mm and a depression depth $h = 28$ mm, the volume of the spherical segment is calculated to be 1269 cm^3. According to the simulation results, the volume of the thermal hotspot confined by the 250^{I} isosolidus (corresponding to 100% solid phase, see Fig. 4b) is of 4208 cm^3. However, this zone contains a shrinkage cavity, porosity, and solid phase.

Assuming feeding from the metal bath lasted up to 180 minutes (see Fig. 4b), the amount of solid phase in the thermal hotspot is approximately 72%, based on the ratio of feeding time to the total solidification duration (250 minutes). Consequently, the shrinkage defects occupy about 28% of the inter dendritic space, yielding an estimated defect volume of 1178 cm^3. This provides a quick method for assessing casting quality without sophisticated measuring equipment or highly qualified personnel.

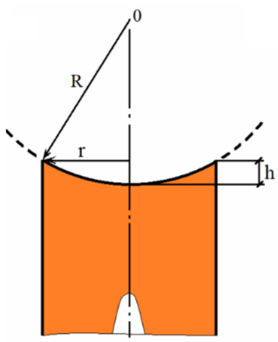

Fig. 7. Scheme for calculating the volume of a shrinkage depression on the top of the riser of a 550-2 mill work roll after electroslag heating (ESH)

For irregularly shaped shrinkage depressions on shaped castings or spheres, the shrinkage depression can be filled with plasticine with further volume calculation by dividing the mass to the density. it can be as the first approximation of the depression volume and the associated shrinkage defects. This allows to calculate the required mass of a chill to eliminate the thermal hotspot and shrinkage cavity, for example, by installing an internal chill.

Based on the results, the term *shrinkage depression* is proposed to be defined as a surface defect in the form of a recess with rounded edges, formed due to low pressure within a hidden shrinkage cavity and contraction of metal on a part of the casting surface with lower strength.

4. Conclusions

1. The formation of hot spots and shrinkage defects in castings can lead to the appearance of a shrinkage depression. Its origin is attributed to low pressure in the center of a shrinkage cavity, where atmospheric pressure causes inward distortion of the already solidified metal surface, especially in the regions with higher temperatures and lower strength.
2. Based on the experimental investigation of the solidification of high-strength cast iron in a roll of ≈2160 kg, the solidification model was adapted for a reference roll. This enabled the model extension to rolls of other sizes.
3. In the example calculation of solidification of cast iron work rolls of ≈7500 kg in a combined metal–sand mold, the positions of isosolidus fronts were determined, as well as the formation of a shrinkage depression on the riser top after electroslag heating, and the corresponding shrinkage cavity volume within the thermal hotspot. The duration of electroslag heating is recommended to be reduced from 250 minutes to 180 minutes. The duration of electroslag heating is recommended to be reduced from 250 minutes to 180 minutes. This is conditioned by the solidification of the upper neck of the roll and the disruption of shrinkage feeding from the metal pool, which also reduced the temperature difference between the upper and lower parts of the roll.
4. A method has been developed to estimate the shrinkage cavity volume in the thermal hotspot based on the shrinkage depression volume. This enables a first-approximation calculation of the required chill mass using known methods, without involving complex instrumentation.
5. A revision to the definition of *shrinkage depression* is proposed: Shrinkage depression – a surface defect in the form of a recess with rounded edges, formed due to low pressure within a hidden shrinkage cavity and contraction of metal on a part of the casting surface with lower strength.

References

[1] DSTU 9051:2020. Iron and steel castings. Defects. Terms and definitions. Effective from 01.04.2021, p. 15. (in Ukrainian).

[2] American Foundry Society. (2007). International Atlas of Casting Defects. ASM International.

[3] Leibenzon, V.O., Pilyushenko, V.L., Kondratenko, V.M., et al. (2009). *Solidification of Metals and Metal Composites: Textbook.* (2nd ed). Kyiv: Naukova Dumka. (in Ukrainian).

[4] Przybyl, J. (1954). *Tuhnuti a nalitkovani odlitku.* Moscow: Machine-Building Literature Publishing House. (in Russian).

[5] Dunphy, R.P., Akerlind, C.G. & Pellini, W.S. (1954). Solidification, feed characteristics of gray cast irons and nodular cast irons. *Foundry*, 82(6), 106.

[6] Khrychikov V.Ye., Semenov O.D., Menyaylo O.V. (2023), Patent of Ukraine No. 127278. Method for eliminating shrinkage cavities in castings with thickened wall sections. (in Ukrainian).

[7] Khrychikov, V., Semenov, A., Meniailo, H., Aftandiliants, Y. & Gnyloskurenko, S. (2022). The process of vacuum formation in the shrinkage cavity at castings crystallization. *Archives of Foundry Engineering*. 22(4), 79-84. https://doi.org/10.24425/afe.2022.143953.

[8] GOST 20426-82. (1983). Non-destructive testing. Radiation methods of defectoscopy. Introduced since 01.07.1983. 15 p. (in Russian).

[9] STP 80.3-015-08 (EN 12680-1:2003). (2008). Casting. Ultrasonic inspection. Steel castings for general use. Kyiv: Ukrainian Center for Conformity Assessment "Prombezpeka". (in Russian).

[10] Reisa, A., Xu, Z., Tol, R.V. & Neto, C.R. (2012). Modelling feeding flow related shrinkage defects in aluminum castings. *Journal of Manufacturing Processes*. 14, 1-7. https://doi.org/10.1016/j.jmapro.2011.05.003

[11] Rafique, M.M.A. & Iqbal, J. (2009). Modeling and simulation of heat transfer phenomena during investment casting. *International Journal of Heat and Mass Transfer*. 52(7-8), 2132-2139. https://doi.org/10.1016/j.ijheatmasstransfer.2008.11.007.

[12] Khrychikov, V.E., Koteshev, N.P., Mushenkov, Y.A. (1987). Method for installing thermocouples in a mold *Soviet Castings Technology*.

[13] Menyaylo, O.V. (2020). *Scientific and Technological Principles of Directional Solidification of Massive Castings from Iron-Carbon Alloys in Combined Molds.* Doctoral dissertation in technical sciences, specialty "Foundry". (in Ukrainian).